

MODELING THE THERMAL PROCESSES OF LASER SYNTHESIS FOR THE NITRIDES IN REFRACTORY METALS

A. A. Uglov, I. Yu. Smurov, and L. V. Karaseva

UDC 336.31:533.211:536.42

We examine the thermal processes which include the motion of phase melt and vaporization fronts in the laser synthesis of nitrides in high-melting refractory metals. The integral radiant flux, on reaching the surface of its target, is determined by a longitudinal x-ray method. We demonstrate that the extreme relationship between the thicknesses of the synthesized layers and the pressure of the gas is a result of the competition between the process of surface vaporization in the region of lower pressures and the increase in the optical density of the beam in the region of higher pressures.

INTRODUCTION

The laser synthesis of the nitrides and carbides of high-melting metals is one of the most promising technological processes [1-3]. The idea behind this method involves the melting of the surface layers of a metal by means of laser emissions and the penetration of alloying components into the melt, these elements in the gaseous (nitrogen, methane, carbon dioxide) [4-7] or liquid phase (liquid nitrogen, pentane, heptane, toluene, and others) [8-10]. The penetration of these alloying elements into the depth of the melt is accomplished by means of thermocapillary convection [11-14], which over a period of time on the order of milliseconds achieves an alloying thickness of about one hundred microns. For a large number of such laser-treatment regimes, characteristic of the elevated pressures of a gas atmosphere, the penetration of the alloying elements occurs throughout the entire depth of the molten layer, i.e., the thicknesses of the synthesized nitride and carbide zones in the high-melting metals do not exceed the depth of the melt layer and in a number of cases are, in fact, determined by the latter. In these particular regimes, the rates of convective mass transfer exceed the velocity of melt-front motion. The foregoing is characteristic of laser pulses in the gas atmosphere of N_2 , CO_2 , and CH_4 for pressures in excess of 3 MPa, when a cluster of laser plasma is formed near the irradiated surface.

A unique feature of laser synthesis under these conditions is the complex time dependence of the radiation flux incident on the metal, and this is associated with the shielding of the flux by the erosion flare and optical discharge. The determination of the integral flow of radiation reaching the surface of the target is accomplished by a longitudinal x-ray method (for example, [15]) which reduces to the measurement of the power of the radiation generated by the laser as a ratio of the radiation passing through the plasma cloud.

We know that under certain conditions the shielding of the laser energy flow by the ejection products or by the plasma near the surface will lead to the appearance of self-oscillations in the system formed by the energy flow and the cloud near the surface, plus the target. This process is not a special case and is characteristic of any concentrated flow of energy, provided that the conditions of self-oscillation excitation are satisfied [16]. The existence of self-oscillation regimes for a change in the temperature of the surface, in the thickness of the welding seam, and in other parameters, was noted in experiments involving the action of an electron beam and laser radiation against various materials.

Under the conditions of laser synthesis of the nitrides in high-melting alloys the self-oscillation processes are characteristic of nitrogen pressures of about 1-8 MPa and of energy-flux densities of $(1.5-3) \cdot 10^{10}$ W/m². According to [17], in this particular case the energy acting on the target can be represented in the form of a series of pulses. The duration of the first radiation pulse is determined by the time to the formation of the plasma cloud and it is equal to 250 μ sec. The remaining pulses exhibit durations of virtually 50 μ sec for an oscillation period of 100 μ sec, and the time interval between the first and second pulses is 125 μ sec.

MATHEMATICAL MODEL

The mathematical model being used here describes the processing of heating, melting, vaporization, and hardening, resulting from the action of an energy flux arbitrarily dependent on time against a metallic plate [18-21]. It is assumed that the absorption of the energy flux is superficial in nature. We take into consideration the radiation and convection losses of heat from both sides of the plate. Under the conditions of the experiment, as a rule, the diameter of the melt zone is considerably greater than its thickness

A. A. Baikov Metallurgy Institute, Academy of Sciences of the USSR, Moscow. Translated from *Inzhenerno-Fizicheskii Zhurnal*, Vol. 60, No. 3, pp. 357-363, March, 1991. Original article submitted November 1, 1989.

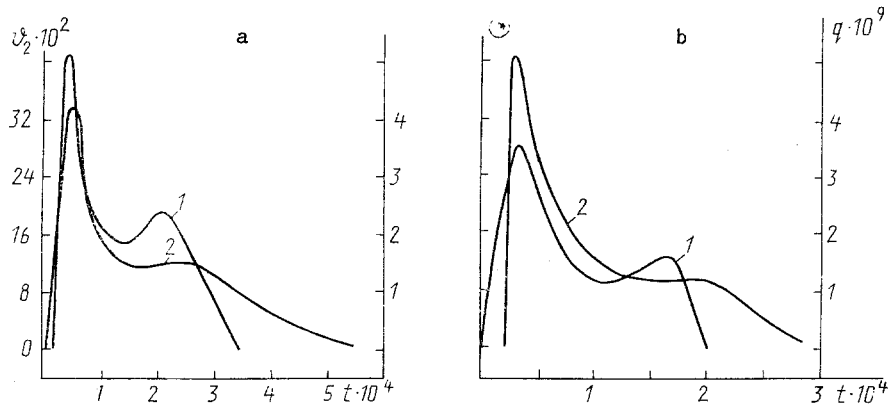


Fig. 1. Absorbed density of the energy flux (1) and the velocity of melt front motion (2) as functions of time: a) $P = 7.4$ MPa; b) 8.5 MPa. $q_0, 10^9$ W/m²; $v_2, 10^{-2}$ m/sec; $t, 10^{-4}$ sec.

and the corresponding Peclet number is considerably smaller than unity [11-14], which allows us to neglect convective heat transfer as small in comparison to conductive transfer and to examine the following one-dimensional problem:

$$\begin{aligned}
 \frac{\partial^2 T_1}{\partial x^2} &= \frac{1}{a_1} \frac{\partial T_1}{\partial t}; \quad S_1(t) < x < S_2(t); \quad t_m < t < \infty; \\
 q_0(t) - \alpha_g [T_1(x, t) - T_g] - \sigma [\epsilon_1 T_1^4(x, t) - \epsilon_g T_g^4] &= -\lambda_1 \frac{\partial T_1}{\partial x} + \\
 &+ \rho_2 L_v \frac{dS_1}{dt}; \quad x = S_1(t); \\
 T_1(x, t = 0) &= T_0; \\
 \frac{dS_1}{dt} &= v_* \exp \left[-\frac{T_*}{T_1(S_1(t), t)} \right]; \\
 \lambda_1 \frac{\partial T_1}{\partial x} &= \lambda_2 \frac{\partial T_2}{\partial x} - \rho_2 L_m \frac{dS_2}{dt}; \quad T_1 = T_2 = T_m; \quad x = S_2(t); \quad S_2(t_m) = 0; \\
 \frac{\partial^2 T_2}{\partial x^2} &= \frac{1}{a_2} \frac{\partial T_2}{\partial t}; \quad S_2(t) < x < l; \\
 -\lambda_2 \frac{\partial T_2}{\partial x} &= \alpha_f (T_2 - T_f) + \sigma (\epsilon_2 T_2^4 - \epsilon_f T_f^4); \quad x = l.
 \end{aligned} \tag{1}$$

The relationships of the thermal vaporization model from [22, 23] have been used in (1), where v_* is a quantity that is close to the speed of sound in the metal; $T_* = L_v A/R$.

System (1) is solved by the method of finite differences (the Cranck–Nicholson scheme with nonlinearity iterations) where the coordinates of the phase transition boundaries are clearly isolated [24, 25]. Into each of these areas (liquid or solid) a movable three-dimensional grid is introduced, the nodes of this grid displacing over time.

We model the action of the energy fluxes against a titanium plate with a thickness of 2 mm, which for the cases considered below serves as a massive body from the standpoint of heat. Analogous calculations are carried out for zirconium.

DISCUSSION OF RESULTS

Figure 1 shows the time dependence of the density of the energy flux incident on the surface of the specimen and the velocity of the melt-front motion in the case of a laser pulse having a duration of approximately a millisecond with a maximum power density of $5 \cdot 10^{10}$ W/m² for nitrogen pressures of $P = 7.4$ and 8.5 MPa within the chamber. The nature of the second maximum on the density curve of the energy flux passing through the plasma cloud is, apparently, analogous to the self-oscillation processes in the system formed by the laser radiation, the surface plasma, and the surface of the target. With a laser pulse of about one millisecond

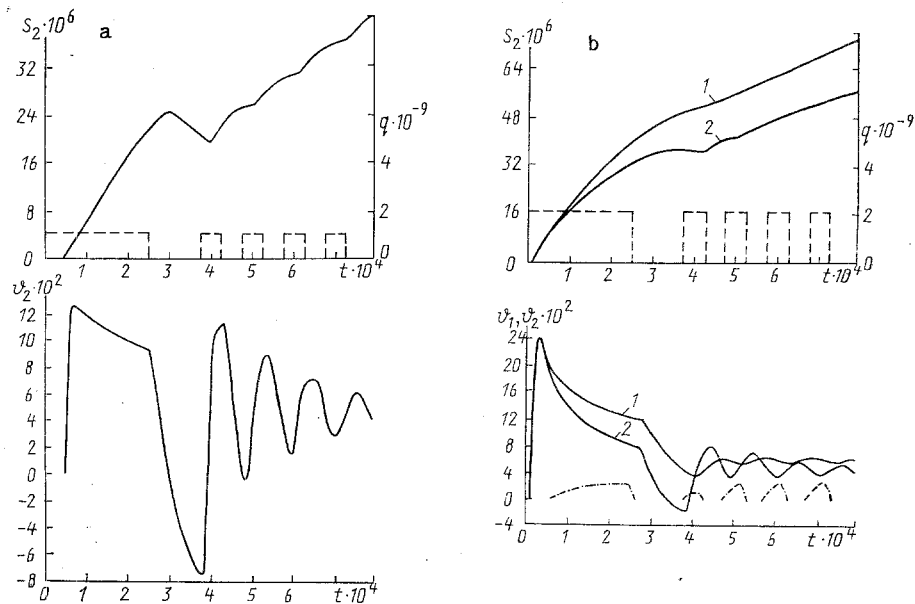


Fig. 2. Coordinate of the melting front, velocities of the vaporization front (dashed—dotted line), and melting rate as functions of time: a) $q_0 = 10^9 \text{ W/m}^2$ (dashed line); b) $2 \cdot 10^9 \text{ W/cm}^2$ (dashed line). $S_2, \text{ m}$; $v_1, v_2, \text{ m/sec}$; $q_0, \text{ W/cm}^2$; $t, \text{ sec}$.

virtually all of the shielding (attenuation of the energy flux by more than a factor of 100) occurs at characteristic time values of $330 \mu\text{sec}$ ($P = 7.4 \text{ MPa}$) and $200 \mu\text{sec}$ ($P = 8.5 \text{ MPa}$), i.e., with an increase in the pressure of the gas the entire smaller fraction of the laser pulse reaches the surface of the target.

Figure 2 shows the coordinates of the melt front S_2 , the melting rates v_2 , and the vaporization rate v_1 , as functions of time, corresponding to the self-oscillation regimes of the laser treatment during the processes of titanium nitride synthesis. The dashed lines in the upper graphs identify the flux density of absorbed energy. Calculations show that on completion of the first pulse the velocity at which the melt front moves initially diminishes to zero, and then changes sign, which indicates the onset of the hardening stage. The oscillation amplitudes in the velocity of melt front motion subsequently diminishes monotonically, and there are no hardening stages (with the exception of a brief interval after the completion of the second pulse, which can be seen in Fig. 2a). This is associated with the storage of energy in the melt layer, when its thickness increases and when it becomes overheated relative to the melting temperature. The velocities of vaporization front motion, determined by the temperature of the surface, are different from zero virtually only at the instant at which the energy flow is effective (see Fig. 2b). The rise in the velocity of the vaporization front motion during the first pulse, as well as the slight increase in the corresponding values for velocity from the second to the fourth pulse, can be ascribed to the rise in the temperature of the heated surface. The velocities v_1 for the motion of the vaporization front are not shown in Fig. 2a, since they are considerably smaller than the corresponding values of v_2 . Among the unique features encountered in the course of the thermal processes in self-oscillation regimes of laser treatment, we should include the noticeable shift in frequency oscillations between the density of the energy flux and the velocity of vaporization front motion, on the one hand, and the velocity of melt front motion on the other hand. In a number of cases, these fluctuations may occur in virtual counterphase (see Fig. 2b).

We can treat the difference between the results of the calculations carried out with consideration of surface vaporization (curves 2 in Fig. 2b) and for the case in which they are neglected (curves 1 in Fig. 2b) as a methodological question. The corresponding values for the temperature of the surface may differ by several factors [18, 19]. The above-indicated differences are sharply diminished as the density of the absorbed energy flux is reduced. Thus, for example, virtually total coincidence is observed for the conditions presented in Fig. 2a.

One of the most significant features of laser synthesis of the nitrides of high-melting metals is the extreme relationship between the thickness of the synthesized layers and the pressure of the nitrogen in the chamber [3, 26], the latter being characterized by an initially sharp increase in the thickness as the pressure of the ambient atmosphere increases, and this is subsequently replaced by a sharp drop in the thickness of the nitride layer, virtually down to its total disappearance. In the nitrogen pressure region greater than 6 MPa the thickness of the synthesized layer is usually equal to the thickness of the melt layer and is determined by the latter.

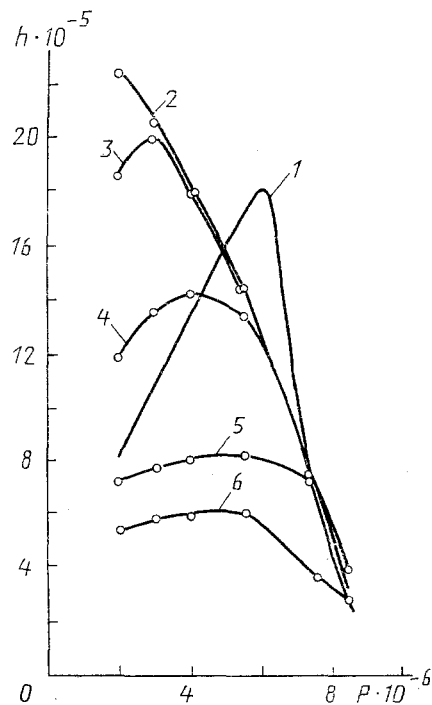


Fig. 3. Thicknesses of the titanium melt (theoretical) layer and the thickness of the synthesized TiN layer, i.e., curve 1 (experiment) as functions of the nitrogen pressure; 2) without consideration of vaporization; $\gamma = 3, -2, -3/4$ for curves 3, 4, and 5; 6) without taking into consideration the relationship between the vaporization rate and the gas pressure. $h, m; P, \text{MPa}$.

This is related to the decisive role played by the convective mass transport of the alloying component [11-14]. Thus, we have the possibility, through modeling of the changes in the depth of the melt, to determine the quantitative relationships governing the changes in the thickness of the synthesized layers as a function of gas pressure.

In the modeling of the above-indicated thermal processes the calculation of metal vaporization in a medium with counterpressure involves considerable difficulty. The problem is of independent interest and goes beyond the scope of the present study. On the other hand, in a number of studies (for example [27, 28]) we find experimental results from the determination of the steady rate of metal vaporization as a function of the pressure in the ambient atmosphere. In these studies the derived results are then approximated by a function of the form P^γ , where $\gamma < 0$, i.e., $v_1(P_1)/v_1(P_2) = (P_1/P_2)^\gamma$. This functional dependence was used by the authors in their calculations, but owing to the difference in the conditions under which the above-described experiments were carried out, in contrast to the conditions of laser synthesis, the calculations were carried out for three different values of γ , equal, respectively, to $-3, -2$, and $-3/4$.

Figure 3 shows the results from a comparison of the calculations to the experimental data from [26]. As follows from these graphs, with a reduction in the exponent for γ (from $-3/4$ to -3) the maximum thickness of the melt layer, increasing in absolute magnitude, shifts into the region of lower pressures. For a better understanding of the features involved in these processes, we also carried out calculations for two extreme cases: the absence of vaporization ($v_1 = 0$), represented by curve 2, and the independence of the vaporization rate from the pressure of the ambient gas (the specific magnitude corresponds to atmospheric pressure), and this case is represented by curve 6. We can see that failure to take into consideration the process of surface vaporization leads to a monotonic relationship between the thickness of the melt layer and the pressure of the surrounding atmosphere; the absence of a maximum on the curve and the significant differences in the region of relatively low pressures indicate the unsuitability of this approach in the pressure region $P < 4 \text{ MPa}$. The foregoing confirms the noticeable influence of vaporization on the thickness of the melt layer under these conditions. On the other hand, in the region of relatively high pressures ($P = 8 \text{ MPa}$) curves 2-5 coincide, and this indicates the virtual absence of vaporization. The analysis that we have carried out here allows us to draw a conclusion to the effect that the extreme dependence of the thicknesses of the synthesized layers on the pressure of the gas can be ascribed to the competing processes of surface vaporization in the region of lower pressures and to an increase in the optical density of the flare in the region of higher pressures. Indeed, with an increase in pressure and a corresponding increase in the optical density of the near-surface plasma we have a reduction in the energy transferred to the target, and this serves to explain

the reduction in the thickness of the melt relative to the extremum as the pressure increases. On the other hand, the increase in the radiative flux density under conditions of developed vaporization leads to a reduction, in these calculations, of the melt layer thickness [20], and in this case this served to explain the reduction in the thickness of the melt layer relative to the extremum that appears with a reduction in pressure. Taking into consideration the reduction in the rate of vaporization as the gas pressure increases, particularly in accordance with the P^γ law, leads to a noticeable increase in the thickness of the melt layer (see curve 6 in Fig. 3), whose maximum values increase as the exponent of γ becomes smaller. Indeed, the lower the energy expended on vaporization, the more energy remains available for the melting of the metal.

CONCLUSIONS

Thus, calculation of the thermal processes in the laser synthesis of the nitrides in high-melting metals, based on a model with two moving phase boundaries, yields qualitative agreement (as well as quantitative agreement in the case of high gas pressures) with experimental results. The differences are a result primarily of the approximate consideration given to the relationship between vaporization and the pressure of the surrounding atmosphere and the failure to take into consideration the heats of TiN formation. In conclusion, let us note certain features in the thermal processes of the laser synthesis in nitrides of high-melting metals as compared to the typical processes of laser pulse treatment. The metal melts primarily only during the initial part of the radiation pulse, which is several times shorter than its overall duration (100-300 μ sec and 1.5 msec). The pulsed-periodic thermal procedure, corresponding to self-oscillation regimes, may lead to characteristic structure-phase changes in the treatment zone, and to the formation of stratified structures [1, 3]. A consequence of the high nitrogen pressure leading to the suppression of vaporization is the formation of a relatively deep melt bath with higher overheating than under ordinary conditions, which leads to an increase in the time within which the melt exists and within which it becomes saturated with the alloying elements. The quantitative relationships analogous to those indicated above are characteristic for the laser synthesis of zirconium nitride.

NOTATION

$T_1(x, t)$ and $T_2(x, t)$, temperature of the liquid and solid phases; x , coordinate; t , time; $S_1(t)$ and $S_2(t)$, coordinates of the vaporization and melt fronts; $q_0(t)$, absorbed density of the energy flux; $a_{1,2}$, coefficients of thermal diffusivity for the liquid and solid phases; $\lambda_{1,2}$, coefficients of thermal conductivity for the liquid and solid phase; $\rho_{1,2}$, density of the liquid and solid phase; $L_{m,v}$, specific heats of melting and vaporization; $\alpha_{g,f}$, coefficient of convective heat losses from the heated side of the plate, and the reverse side; $\epsilon_{1,2}$, emissivities of the heated and reverse sides of the plate; $\epsilon_{g,f}$, emittances of the ambient medium near the heated and reverse sides of the plate; T_m , melting point; T_0 , initial temperature of the plate; t_m , time of melt onset; l , plate thickness; A , atomic weight of plate material; R , universal gas constant.

LITERATURE CITED

1. N. N. Rykalin, A. A. Uglov, I. V. Zuev, and A. N. Kokora, *Laser and Electron Treatment of Materials. Handbook* [in Russian], Moscow (1985).
2. N. N. Rykalov and A. A. Uglov, *Kvant. Élektron.*, **8**, No. 6, 1193-1202 (1981).
3. N. N. Rykhalin and A. A. Uglov, *FKhOM*, No. 4, 3-9 (1985).
4. R. V. Arutyunyan, V. Yu. Baranov, A. A. Bol'shov, et al., *Poverkhnost'*, No. 9, 5-12 (1986).
5. A. L. Galiev, L. L. Krapivin, L. I. Mirkin, et al., *Dokl. Akad. Nauk SSSR*, **251**, No. 2, 336-338 (1980).
6. A. A. Uglov, A. F. Gorbach, I. Yu. Smurov, et al., *FKhOM*, No. 2, 3-8 (1986).
7. A. A. Uglov, M. B. Ignat'ev, A. G. Gnedovets, and I. Yu. Smurov, *J. Physique*, **50**, C-5, No. 5, 727-733 (1989).
8. S. A. Astapchik and T. N. Khat'ko, *Vestsi Akad. Nauk BSSR, Ser. Fiz.-Tekhn. Navuk*, No. 3, 30-33 (1986).
9. S. A. Astapchik and T. N. Khat'ko, *Vestsi Akad. Nauk BSSR, Ser. Fiz.-Tekhn. Navuk*, No. 2, 24-28 (1987).
10. S. A. Astapchik and T. N. Khat'ko, *Izv. Akad. Nauk SSSR, Ser. Fiz.*, **51**, No. 6, 1221-1224 (1987).
11. A. A. Uglov, I. Yu. Smurov, A. G. Gus'kov, et al., *Izv. Akad. Nauk SSSR, Ser. Fiz.*, No. 1, 155-162 (1988).
12. A. G. Gus'kov, I. Yu. Smurov, and A. A. Uglov, *Izv. Akad. Nauk SSSR, Mekh. Zhidk. Gaza*, No. 1, 155-162 (1988).
13. A. A. Uglov, I. Yu. Smurov, A. G. Gus'kov, et al., *Teplofiz. Vys. Temp.*, No. 1, 155-162 (1988).
14. A. A. Uglov, I. Yu. Smurov, I. K. Tagirov, et al., *FKhOM*, No. 6, 24-29 (1988).
15. A. A. Uglov and M. B. Ignat'ev, *Fizika Plazmy*, **8**, No. 6, 1285-1290 (1982).
16. A. A. Uglov and S. V. Selishchev, *Self-Oscillation Processes under Concentrated Flows of Energy* [in Russian], Moscow (1987).
17. A. A. Uglov, I. Yu. Smurov, M. B. Ignat'ev, et al., *FKhOM*, No. 3, 18-20 (1986).
18. A. A. Uglov, I. Yu. Smurov, and A. M. Lashin, *Teplofiz. Vys. Temp.*, **27**, No. 1, 87-93 (1989).

19. I. Yu. Smurov and A. M. Lashin, in: *Physical Chemical Processes of Treating Materials with Concentrated Flows of Energy* [in Russian], Moscow (1989), pp. 160-169.
20. A. M. Lashin, I. Yu. Smurov, A. A. Uglov, P. Matteazzi, and V. Tagliaferri, *Int. J. Heat and Technology*, **7**, No. 2, 60-73 (1989).
21. A. A. Uglov, I. Yu. Smurov, A. M. Lashin, and A. G. Gnedovets, in: *High-Temperature Dust-Laden Gets in Plasma Technology*, Utrecht, The Netherlands (1989), pp. 463-486.
22. S. I. Anisimov, Ya. A. Imas, G. S. Romanov, and Yu. V. Khodyko, *The Effect of High-Power Radiation on Metals* [in Russian], Moscow (1970).
23. S. I. Anisimov, A. M. Bonch-Bruevich, M. A. El'yashevich, et al., *Zh. Tekh. Fiz.*, **36**, No. 7, 1273-1277 (1966).
24. M. A. Hastaoglu, *Int. J. Heat Mass Transfer*, **29**, No. 3, 495-499 (1986).
25. J. G. Blom, J. M. Sanz-Serna, and J. G. Verwer, *J. Comput. Phys.*, **74**, 191-213 (1988).
26. A. A. Uglov, M. B. Ignat'ev, and I. Yu. Smurov, *FKhOM*, No. 2, 88-91 (1987).
27. J. S. Haggerty, D. W. Lee, and J. F. Wenckus, AFML-TR-68-288 (1968).
28. S. Otani, T. Tanaka, and Y. Ishizawa, *J. Mater. Sci.*, **21**, 176-178 (1986).

THERMAL RESISTANCE OF THE VAPORIZATION ZONE FOR A HEAT TUBE WITH A THREADED CAPILLARY SYSTEM

I. M. Blinchevskii and S. P. Ermolaev

UDC 536.242

We present theoretical relationships with which to estimate the thermal resistance of the vaporization zone in a low-temperature heat tube with a capillary structure in the form of threading on the inside surface of the frame.

A threaded capillary structure (CS) allows us to achieve high heat-flux density in the vaporization zone, and it is simple from a technological standpoint. This type of CS has therefore gained widespread acceptance in arterial heat tubes (HT). A number of studies [1-4] has been devoted to the determination of thermal resistances in threaded CS. However, no consideration was given in these studies to the actual thread geometry nor to the influence of the heat flow on thermal resistance. In a number of cases, the assumptions based on the derivation of relationships for the calculation of thermal resistance failed to take into consideration contemporary concepts regarding meniscus vaporization. It is the goal of the present study to investigate the thermal resistance of the vaporization zone in a HT with a threaded CS, with consideration given to the above-indicated factors. The lateral cross sections of these variants of arterial HT can be seen in Fig. 1a, b, with the threading profile shown in Fig. 1c. The fluid at the edge of the meniscus can be divided into three characteristic regions [5]: the equilibrium film, a vaporization zone, and the meniscus itself. The adhesion forces in the equilibrium film, a consequence of the interaction between the molecules of the fluid and the wall, are so great that the fluid does not vaporize. In the vaporization film, whose thickness is greater than that of the equilibrium film, the adhesion forces diminish and vaporization becomes possible. The adhesion forces beneath the actual meniscus become negligibly small, and the flow of the fluid can be ascribed to the capillary pressure gradient generated by the change in the curvature of the meniscus. This change is slight in comparison to the change of curvature in the vaporization film, where it is altered by factors of ten. Let us determine that segment $k-a$ of the actual meniscus and the corresponding angle $(\varphi_k - \varphi_a)$, i.e., see Fig. 1c, making the following assumptions: the flow is laminar, the radius of the meniscus within the limits of the angle $(\varphi_k - \varphi_a)$ changes only by 5%, and the change in the rate of flow and in the lateral cross section of the fluid flow between sections $k-k_1$ and $a-o_2$, owing to vaporization and the change in the radius of the meniscus, is small, while the density of the heat flow in the vaporization zone is constant. Under these assumptions, the pressure losses due to friction in the flow of the fluid along the segment $x_{k_1}-x_{o_2}$:

$$\Delta p_{k-o_2} = B \int_{x_{k_1}}^{x_{o_2}} \frac{dx}{y^3}, \quad (1)$$

Translated from *Inzhenerno-Fizicheskii Zhurnal*, Vol. 60, No. 3, pp. 363-368, March, 1991. Original article submitted December 21, 1989.